Distribution Category:
LMFBR -- Physics: Base
Technology (UC-79d)

ANL-87-5

ANL--87-5

DE87 005942

ARGONNE NATIONAL LABORATORY
9700 South Cass Avenue
Argonne, Illinois 60439

$^{235}U(n,f)$, $^{238}U(n,\gamma)$, $^{238}U(n,f)$ and $^{239}Pu(n,f)$ REACTION RATE MEASUREMENT CALIBRATIONS AT ZPPR

by

W. P. Poenitz, D. W. Maddison, J. M. Gasidlo
S. G. Carpenter and R. J. Armani

Applied Physics Division

January 1987

DISCLAIMER

This report was prepared as an account of work sponsored by an agency of the United States Government. Neither the United States Government nor any agency thereof, nor any of their employees, makes any warranty, express or implied, or assumes any legal liability or responsibility for the accuracy, completeness, or usefulness of any information, apparatus, product, or process disclosed, or represents that its use would not infringe privately owned rights. Reference herein to any specific commercial product, process, or service by trade name, trademark, manufacturer, or otherwise does not necessarily constitute or imply its endorsement, recommendation, or favoring by the United States Government or any agency thereof. The views and opinions of authors expressed herein do not necessarily state or reflect those of the United States Government or any agency thereof.

MASTER

DISTRIBUTION OF THIS DOCUMENT IS UNLIMITED

TABLE OF CONTENTS

LIST OF FIGURES

LIST OF TABLES

LIST OF TABLES (cont'd)

Page No.

$^{235}U(n,f)$, $^{238}U(n,\gamma)$, $^{238}U(n,f)$ and $^{239}Pu(n,f)$ REACTION RATE MEASUREMENT CALIBRATIONS AT ZPPR

W. P. Poenitz, D. W. Maddison, J. M. Gasidlo,
S. G. Carpenter and R. J. Armani

ABSTRACT

New reference deposits for ^{235}U, ^{239}Pu and ^{238}U have been established with mass uncertainties of <0.2%. These new deposits replace the older reference deposits which were used during the last 17 years and improve the uncertainty of reaction rate measurements due to reference mass uncertainties by about a factor of 6. Measurements of the fission fragment absorption in 2π geometry have been made for these deposits using a new technique of comparing 2π and low-geometry count rates.

Two measurements of the ^{238}U capture rate in depleted uranium samples based upon the thermal cross sections of $^{238}U(n,\gamma)$, $^{235}U(n,f)$ and $^{239}Pu(n,f)$ and based upon the ^{243}Am calibration technique confirm the ZPPR measurement technique within the quoted uncertainty of ± 0.5%.

I. INTRODUCTION

Spatial distributions of reaction rates of $^{235}U(n,f)$, $^{238}U(n,\gamma)$, $^{238}U(n,f)$, $^{239}Pu(n,f)$, as well as reaction rate ratios, are measured on a regular basis in ZPPR fast-critical assemblies. These measurements are usually done with metallic foils and subsequent analysis of decay gamma rays. The calibration factors for the gamma detectors were obtained by measurements relative to fissile or fissionable deposits of known mass and for $^{238}U(n,\gamma)$ by measuring the gamma intensities of ^{243}Am sources for which the decay rates are accurately known from alpha spectroscopy. A detailed description of the techniques used in this context in the past has been given recently.[1]

The present report describes improvements of the basic calibration techniques for the reaction rate determinations, which were considered desirable in view of recent advances in ^{235}U and ^{239}Pu sample mass determinations[2,3] and in view of some inconsistencies found in recent intercomparisons of reaction rate measurements.[4] Fission fragment absorption, which contributes to the uncertainty of the calibration factors has also been investigated.

New sets of ^{235}U, ^{238}U and ^{239}Pu reference deposits were prepared by molecular (uranium) or electro (plutonium) deposition techniques on 0.0127 cm thick stainless steel discs. The deposits were ~1.78 cm in diameter and ~40 to 70 $\mu g/cm^2$ in thickness. Also included in the present measurements were the previously used reference deposits, a ^{239}Pu

reference deposit from ZPR at Argonne National Laboratory - East, as well as two ^{235}U deposits obtained from the Chemistry Division, AERE, Harwell. The old reference deposits had been involved in various intercomparisons[4,5] and in those described in Ref. 1. The latter three samples were used in other recent intercomparisons.[3]

The masses were determined by absolute measurements of the alpha decay rates and the known specific activity of the materials. This is described in Section II. Samples from each set were sent to three different laboratories (two each of ^{235}U, ^{238}U, and ^{239}Pu) where their masses were determined by the isotopic dilution technique. These values are quoted in Section II. The determination of the fission fragment absorption is described in Section III. Relative mass determinations by fission counting is described in Section IV. The various determinations of the deposit masses and of the mass ratios represent an overdetermination and final values for the sample masses were obtained from a generalized least-squares fit which is described in Section V.

Determinations of the ^{238}U capture rate relative to $^{235}U(n,f)$ and $^{239}Pu(n,f)$ in a thermal neutron field are described in Section VI. Updated values for various techniques relative to the standard ^{243}Am technique are also given in this section.

II. DETERMINATION OF THE FISSILE AND FISSIONABLE DEPOSIT MASSES

A. Mass Determination Based Upon Specific Alpha Activities and Absolute Alpha Decay Rates

The determination of the masses of fissile and fissionable deposits based upon their isotopic composition and actinide half-lives, which yield the specific activities, and measurements of their absolute alpha decay rate has been in use for a long time. However, only since the actinide half-lives have become known very well[6] can masses be determined by this technique with uncertainties comparable to those obtained from destructive analysis.

The fissile material used for the new ^{235}U reference deposits was originally high purity ^{235}U which was spiked with ^{234}U.[7] This material was involved in a recent international ^{235}U sample mass intercomparison and has been described in detail in associated reports.[3] However, a new determination of its isotopic composition has been made by the Analytical Group of the Chemical Technology Division of Argonne National Laboratory which is independent of NBS standards[8] and improved the agreement between the values obtained for the specific activity based upon actinide half-lives and other techniques. Current values for this material are given in Table I.

The data given in Table I for the old ^{235}U reference deposits have been obtained from internal memoranda. The uncertainty for the ^{234}U content of this material is 1% which is consistent with the scatter of values obtained for a similar material at about the same time as these deposits were made (in 1968). The values for the ^{235}U deposits from AERE are those cited in Ref. 3.

TABLE I. Isotopic Compositions and Specific Activities of the U Deposits

Sample Identifications	Isotopic Composition, wt%				Specific Activities, αpmpμgr			
Atomic Weight	^{234}U 234.04	^{235}U 235.04	^{236}U 236.05	^{238}U 238.05	Isotopic Dilution	Isot. Comp., Half Lives	Colorimetry	Average
NEW5-01-16 (New Reference Deposits)	1.0203 (5)[a]	98.4409 (20)	0.4392 (5)	0.0996[b] (5)	146.24[c] (25)	146.16 (28)	146.1 (9)	146.20 (18)
OLD5- -8,-19,-22,-23 (Old Reference Deposits)	1.045	93.28	0.287	5.38		149.2 (1.5)		149.2 (1.5)
HAR -U5,A,B (see Ref. 3)	1.1104	92.409	0.315	6.165		158.3 (5)		158.3 (5)
NEW8-01-16	0.0000997[d] (5)	0.01393 (5)	0.0000 (5)	99.9863[b] (20)		0.7606		

[a]Values in brackets give the uncertainties for corresponding digits.

[b]Isotopic composition from ANL-East, Chemical Technology Division

[c]Value based on an isotopic dilution determination made in 1974, independent from the isotopic dilution measurements in the present report.

[d]Value from present alpha spectroscopy.

The fissionable material used for the new ^{238}U reference deposits is a high purity ^{238}U and 98.1% of its alpha activity is due to ^{238}U decay. The contribution to the alpha decay rate from its ^{235}U content is very small (0.1%). Though the ^{234}U content is very low (0.0001 atom %) its contribution to the alpha decay rate is 1.8%. The absolute decay rate determination of the ^{238}U deposits was based upon 2π alpha counting, thus this contribution needs to be known accurately. Because of its low content, the ^{234}U atom percent could not be obtained with sufficient accuracy from isotopic mass spectroscopy and has been measured by alpha spectroscopy instead. For this purpose, the ^{238}U samples were placed ~3 mm from the surface of a surface barrier detector and their alpha spectra were recorded. Though the resolution in this geometry was far inferior to that obtained with more conventional sample-detector separations, a clear separation of the ^{234}U alphas from the ^{238}U alphas and from most of the ^{235}U alphas was obtained as can be seen in Fig. 1. The contribution from the ^{234}U alpha decay was determined to be 1.81 ± 0.01% based on 15 samples measured with a χ^2 per degree of freedom of 0.62. The data on the ^{238}U material are also given in Table I.

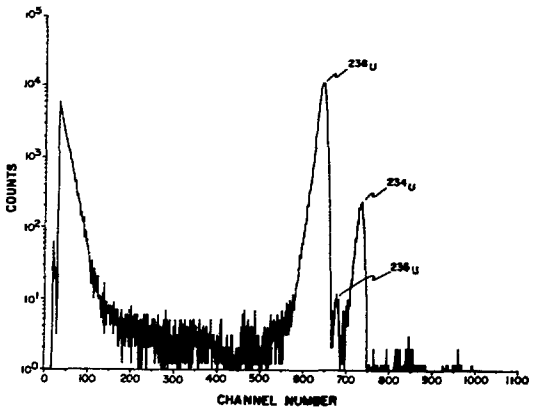

Fig. 1. ^{238}U Deposit Alpha Spectrum

The fissile material for the new ^{239}Pu deposits was selected to reduce the contributions of fission in other isotopes relative to the old reference deposits. The data on the three ^{239}Pu materials involved are given in Table II. The alpha decay rate is always dominated by the decay of ^{239}Pu for which the isotopic weight percent is known with negligible uncertainty because of its high content. Therefore, the uncertainties of the specific activities are entirely due to the uncertainty of the ^{239}Pu half-life which is ~0.1%.[6] Impurities of ^{238}Pu and ^{241}Am could easily be excluded from the alpha decay rate based upon alpha spectroscopy.

The alpha decay rates of the ^{235}U and ^{239}Pu samples were measured with low geometry counters at ANL-East and ANL-West. Both counters were based on the same design which has been described in Refs. 3 and 4. However, the geometry of the counter has been measured independently in both laboratories (aperture diameter, aperture to shelf distance). An advantage of these counters is the use of surface barrier detectors which permits the recording of the alpha spectra. This in turn allows the exclusion of most impurities and provides other useful information discussed in Section III. Typical spectra obtained for the new ^{235}U and ^{239}Pu reference deposits are shown in Figs. 2 and 3, respectively. The alpha decay rates of the ^{239}Pu samples have been measured repeatedly with geometry factors of ~1/1022 and 1/2292 (second and third shelf). The shelf dependence of the absolute decay rates has been investigated with

TABLE II. Isotopic Compositions and Specific Activities of the Pu Deposits

Sample Identifications	Isotopic Composition, wt%				Specific Activities, αpsμgr	
	^{239}Pu	^{240}Pu	^{241}Pu	^{242}Pu	Isotopic	Isot. Comp.,
Atomic Weight	239.05	240.05	241.06	242.06	Dilution	Half Lives
NEW9-01-17 (New Reference Deposits)[c]	98.973 (3)[a]	1.009 (2)	0.018[b] (2)			2356.3 (2.9)
Pu239-ZPR#1[c]	98.939	1.012	0.0491		2359.3 (11.8)	2360.2 (2.9)
OLD9-65, -70[c]	94.414	5.264	0.307	0.016		2609.1 (2.9)

[a]Values in brackets give the uncertainties in the corresponding last digits.

[b]Isotopic composition is the average of four determinations.

[c]Material also contains ^{241}Am and ^{238}Pu.

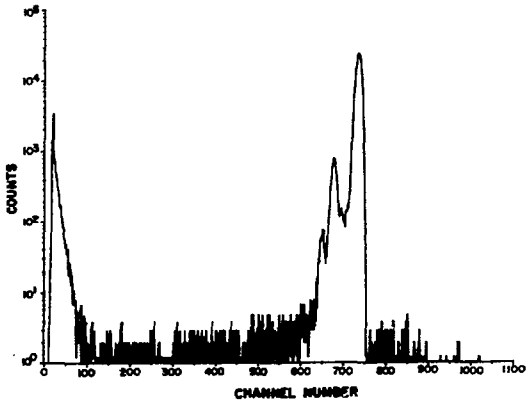

Fig. 2. ^{235}U Deposit Alpha Spectrum

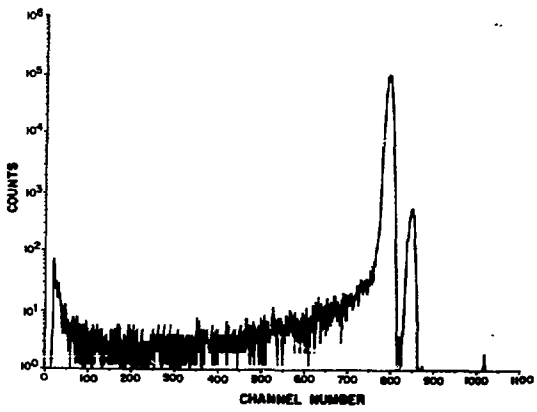

Fig. 3. ^{239}Pu Deposit Alpha Spectrum

measurements on the first to fourth shelf for several ^{239}Pu deposits. This revealed a bias of ~0.2% for measurements on the first shelf which was attributed to inhomogeneity of the deposits and sample backing warping. A corresponding correction has been applied to the ^{235}U decay rates which were exclusively measured on the first shelf because of their lower decay rates.

The alpha decay rates of the ^{238}U deposits were determined in a 2π gas proportional counter. The efficiency of the counter as a function of deposit thickness was known from prior measurements with ^{235}U deposits relative to low geometry counter measurements.[9] The alpha decay rates for the ^{235}U, ^{239}Pu and ^{238}U deposits are given in Tables III, IV and V, respectively. For ^{239}Pu these exclude the contributions from the ^{241}Am and ^{238}Pu impurities, for ^{238}U they include the ^{234}U and ^{235}U contributions. The statistical uncertainties have been replaced with one half of the difference between the measurements at ANL-East and ANL-West, whenever it was found to be larger, in order to account for reproducibility. The alpha decay rates of the ^{238}U deposits are from measurements at ANL-East only.

Additional measurements of the alpha decay rates of the ^{235}U samples were made in a 2π proportional counter. These measurements should be independent of sample inhomogeneity and backing warping. However, in order to exclude effects due to the choice of the plateau voltage and to obtain values independent of the low geometry counter, these values have been taken as relative to the decay rate of one of the deposits. The results of these relative decay rates are given in Table VI.

Absolute deposit masses were derived from the absolute alpha decay rates given in Tables III-V and the specific activities given in Tables I and II. These values are given in Tables VII-IX. The total uncertainties for the masses consist of the statistical uncertainties or reproducibilities given in Tables III to V; 0.1% for the low-geometry counter geometry for second and lower shelves, 0.2% for the first shelf;

TABLE III. Alpha Decay Rates of the ^{235}U Deposits

Sample	Decay Rate, αpm	Statistical Uncertainty, %	Total Uncertainty, %
NEW5-01	17,539	0.15	0.27
02	17,815	0.10	0.24
03	17,629	0.10	0.24
04	17,090	0.15	0.27
05	24,577	0.15	0.27
06	24,369	0.10	0.24
07	24,302	0.10	0.24
08	24,142	0.10	0.34
09	24,136	0.09	0.24
10	24,166	0.09	0.24
11	23,709	0.20	0.30
12	18,041	0.07	0.23
13	24,182	0.30	0.37
14	24,100	0.35	0.42
15	22,915	0.07	0.23
16	24,075	0.25	0.34
OLD5-08	12,958	0.10	0.24
19	16,527	0.10	0.24
22	15,980	0.14	0.26
23	15,952	0.14	0.26
HAR-A	54,855	0.10	0.24
B	54,890	0.10	0.24

TABLE IV. Alpha Decay Rates of the ^{239}Pu Deposits

Sample	Decay Rate, αps	Statistical Uncertainty, %	Total Uncertainty, %
NEW9-05	251,582	0.10	0.17
06	236,926	0.10	0.17
07	253,060	0.05	0.15
08	241,701	0.05	0.15
09	272,251	0.05	0.15
10	261,732	0.05	0.15
11	274,161	0.05	0.15
12	276,507	0.05	0.15
13	358,735	0.03	0.14
14	196,816	0.10	0.17
15	249,127	0.05	0.15
16	255,149	0.10	0.17
17	219,791	0.05	0.15
ZPR-01	191,299	0.07	0.16
OLD9-65	279,979	0.07	0.16
70	279,950	0.07	0.16

TABLE V. Alpha Decay Rates of the ^{238}U Deposits

Sample	Decay Rate, αpm	Statistical Uncertainty, %	Total Uncertainty, %
NEW8-01	103.56	0.10	0.17
02	99.80	0.10	0.17
03	100.26	0.10	0.17
04	98.89	0.10	0.17
05	98.99	0.10	0.17
06	97.30	0.10	0.17
07	97.75	0.10	0.17
08	98.32	0.10	0.17
09	98.01	0.10	0.17
10	94.12	0.10	0.17
11	100.46	0.10	0.17
12	97.92	0.10	0.17
13	98.72	0.10	0.17
14	98.02	0.10	0.17
15	99.77	0.10	0.17
16	98.44	0.10	0.17

TABLE VI. Alpha Decay Ratios for ^{235}U Samples

Samples Rel. to -01	Ratio[a]
NEW5-02	1.0156 ± 0.0025
-03	1.0075 ± 0.0025
-04	0.9799 ± 0.0024
-05	1.3998 ± 0.0037
-06	1.3903 ± 0.0037
-07	1.3890 ± 0.0037
-08	1.3839 ± 0.0037
-09	1.3779 ± 0.0037
-10	1.3786 ± 0.0037
-11	1.3534 ± 0.0036
-12	1.0313 ± 0.0025
-13	1.3776 ± 0.0037
-14	1.3707 ± 0.0037
-15	1.3103 ± 0.0035
-16	1.3686 ± 0.0036

[a]The uncertainty consists of 0.1% for counting statistics, 0.1% for counting statistics of NEW5-01 (totally correlated), 0.1% for scattering and absorption correction for ratios of ~1.3, and 0.2% for reproducibility (plateau stability).

TABLE VII. Masses of the ^{235}U Samples, μg U

Sample	ANL-W	ANL-E(CT)	ANL-W(AL)	NBL	Ref. 3[a]
NEW5-01	119.97 ± 0.34				
-02	121.85 ± 0.32				
-03	120.58 ± 0.32				
-04	116.89 ± 0.33				
-05	168.11 ± 0.48				
-06	166.68 ± 0.43				
-07	166.22 ± 0.43				
-08	165.13 ± 0.43		166.10 ± 0.34		
-09	165.09 ± 0.43		165.64 ± 0.26		
-10	165.29 ± 0.43				
-11	162.17 ± 0.51				
-12	123.40 ± 0.31				
-13	165.40 ± 0.64	165.02 ± 0.22			
-14	164.84 ± 0.70	164.48 ± 0.21			
-15	156.74 ± 0.39			156.79 ± 0.28	
-16	164.67 ± 0.57			164.28 ± 0.30	
OLD5-8	86.85 ± 0.89				
-19	110.77 ± 1.14				
-22	107.10 ± 1.11				
-23	106.92 ± 1.11				
HAR-A	346.53 ± 1.10				346.4 ± 0.6
B	346.75 ± 1.10				347.2 ± 0.7

[a]From least-squares fit of Ref. 3.

TABLE VIII. Masses of the ^{239}Pu Samples, μg Pu[a]

Sample	ANL-W[b]	ANL-E(CT)	ANL-W(AL)
NEW9-05	106.77 ± 0.23		
-06	100.55 ± 0.21		
-07	107.40 ± 0.21		
-08	102.58 ± 0.20		
-09	115.54 ± 0.22		
-10	111.08 ± 0.21		111.42 ± 0.20
-11	116.35 ± 0.23		
-12	117.35 ± 0.23		117.76 ± 0.18
-13	152.25 ± 0.29		
-14	83.53 ± 0.18	83.57 ± 0.13	
-15	105.73 ± 0.20	105.81 ± 0.16	
-16	108.28 ± 0.23		
-17	93.28 ± 0.18		
ZPR-01	31.06 ± 0.16		
OLD-65	107.31 ± 0.21		
-70	107.30 ± 0.21		

[a]Values obtained by isotopic dilution from NBL for NEW9-16 and -17 were grossly discrepant and are not shown here.

[b]Total uncertainty based on 0.1% uncertainty for statistics and reproducibility, 0.1% for counter geometry, 0.1% for sample inhomogeneity and backing warping, and 0.12% for the specific activity.

TABLE IX. Masses of the ^{238}U Samples, μg U

Sample	ANL-E/W	ANL-E(CT)	ANL-W(AL)	NBL
NEW8-01	136.16 ± 0.28			
-02	131.21 ± 0.27			
-03	131.82 ± 0.27			
-04	130.02 ± 0.27			
-05	130.15 ± 0.27			
-06	127.93 ± 0.26			
-07	128.52 ± 0.26			
-08	129.27 ± 0.27			
-09	128.86 ± 0.26			
-10	123.74 ± 0.25		125.38 ± 0.98	
-11	132.08 ± 0.27		133.83 ± 0.22	
-12	128.74 ± 0.26			
-13	129.79 ± 0.27	130.29 ± 0.20		
-14	128.87 ± 0.26	129.41 ± 0.20		
-15	131.17 ± 0.27			131.40 ± 0.24
-16	129.42 ± 0.27			129.21 ± 0.23

0.1% for sample inhomogeneity and backing warping; and the uncertainties of the specific activities given in Tables I and II. For the ^{238}U masses, the additional systematic uncertainties are 0.2% for the efficiency of the 2π proportional counter and 0.1% for the plateau stability. The total uncertainties for the relative alpha decay rates of Table VI consist of the given statistical uncertainties, 0.1% for background, 0.2% for plateau stability, and 0.1% for efficiency differences where deposit thicknesses differed.

B. Masses Determined by the Isotopic Dilution Analysis

Two samples of each material were analyzed by mass spectrometric isotopic dilution analysis by the Analytical Chemistry Laboratory of the Chemical Technology Division of ANL-East (ANL-E (CT)), by the Analytical Chemistry Laboratory of ANL-West (ANL-W (AL)), and by the New Brunswick Laboratory (NBL). These analyses typically consisted of adding weighed aliquots of National Bureau of Standards (NBS) standards of the same element but different isotopic compostion to the material which was disolved from the backings. Subsequent mass isotopic spectrometric assay provided the unknown masses based upon the mass of the added NBS standard and the isotopic compositions of the original material and the spike. The results from these analyses are also given in Tables VII-IX. The same NBS standards have been used in some of the analyses which results in correlations of some of the uncertainties. This can be seen in Table X. The uncertainties of the results from ANL-E(CT) have been restated to represent 1σ values, and the uncertainties for the NBL data have been estimated assuming that they are similar as for the ANL-E(CT) and ANL-W(AL) values.

III. FISSION FRAGMENT ABSORPTION

Total fission fragment absorption for fission in an isotropic neutron field or for isotropic fission fragment angular distributions is commonly corrected for with an efficiency factor

$$\varepsilon = 1 - \frac{t}{2R}$$

TABLE X. Standards Used for the Isotopic Dilution Analyses by the Different Laboratories

	U235	U238	Pu239
NBL	NBS995(U-233)	NBS995(U-233)	NBS996(Pu-244)
ANL-E(CT)	NBS950a(U-238)	NBS993(U-235)	NBS996(Pu-244)
ANL-E(AL)	NBS960(U-NAT)	NBS960(U-NAT)	NBS949(Pu-242)

where t is the deposit thickness in mg/cm^2 and R is the range of the fission fragments in the deposit material in mg/cm^2. The range of fission fragments has been measured for various materials[10,11] and can be approximated with

$$R \approx 0.67 \cdot \sqrt{A} \qquad \text{for} \quad A < 197, \text{ and}$$

$$R \approx 0.65 \cdot \sqrt{A} \qquad \text{for the actinides,}$$

where A is the atomic weight.

For composite materials, C, it is common to apply Bragg's rule:

$$R_c = \left[\sum_i \frac{A_i}{A_c} \frac{1}{R_i} \right]^{-1} .$$

The above formula for the fission fragment counting efficiency is based upon the assumption of an infinite and homogeneous deposit on an ideally flat and smooth backing. However, macroscopic and microscopic (clumping) inhomogeneities of the deposit and fine-structure of the backing affect the total fission fragment absorption. Additional problems come from the usually poor knowledge of the chemical composition of the deposit. Various deposition techniques may deposit impurities as well (sputtering techniques) or the composition of the deposit may change by conversion (e.g., $UO_2 \rightarrow U_3O_8$) or absorption (e.g., $ThO_2 \rightarrow ThO_2 \cdot H_2O$).

Most measurements of fission fragment absorptions have been done by extrapolating the relative fission rates of deposits of different thickness as determined by their alpha decay rate to zero thickness (e.g. Ref. 12 and 13). This technique ignores the effect of the backing which should be largest for very thin deposits and thus affects the extrapolation procedure. A more recent measurement of the fission fragment absorption utilized a special gridded ion chamber which permitted the determination of the angular distribution of the detected fission fragments.[14] The effective fission fragment ranges inferred from such measurements range from agreement with the above formulae to substantial differences (10-20%). Thus, it was considered important to determine experimentally the fission fragment absorption of the deposits involved in the current measurements.

The technique used and described below did not permit the determination of the fission fragment absorption for all of the 54 samples involved. Two relative indicators for the fission fragment absorption were used to relate the values measured for four deposits to the remaining deposits. The first of these indictors is the width of the alpha transitions measured with the surface barrier detector. This width has been found empirically to be linearly related to the effective fission fragment range.[3] Figure 4 shows a comparison between the alpha spectra of two ^{239}Pu deposits which have very similar thicknesses. The slightly thinner deposit #10 has a substantially broader alpha peak than the

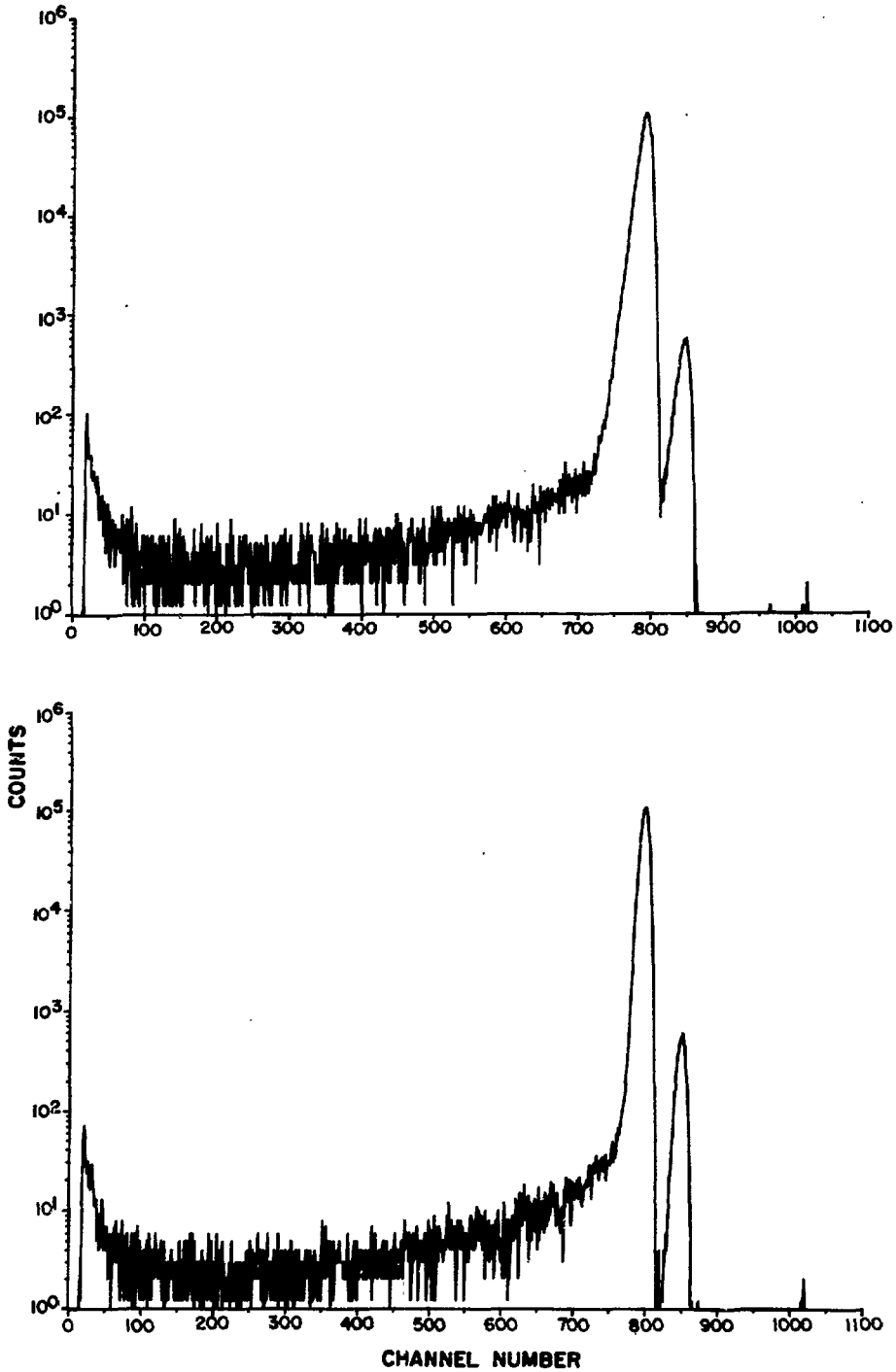

Fig. 4. Comparison of the Alpha Peak Widths for Two ^{239}Pu Deposits of Similar Thicknesses (#10 above and #9 below)

deposit #9 which indicates differences in microscopic clumping and correlated differences in fission fragment absorption can be expected.

The number of fission fragments below the geometrical cut-off determined by the deposit to collector plate distance has been suggested as another relative measure for the total fission fragment absorption.[3] These pulses are due to fission fragments which are emitted close to 90° relative to the deposit normal and thus lose most of their energy. Being close in energy loss and in angle to those fission fragments which are totally absorbed, they should give a good relative measure for the total fission fragment absorption. Figure 5 shows a comparison of the fission fragment pulse height spectra obtained for two deposits. Again, though the deposits have similar thicknesses, the number of the pulses below the geometrical cut-off differ substantially and indicate differences in fission fragment absorption.

A special fission chamber was designed for the measurement of the fission fragment absorption. The chamber is shown schematically in Fig. 6. The chamber is symmetric to its mid-plane and both halves can be operated as ionization counters or as a low-geometry counters. One half of the counter was always operated as an ionization chamber with a ^{235}U deposit which served as a monitor. The collector plate on the other half had a circular opening with four thin wires providing for a more even electrical field. This arrangement permits switching from 2π (ionization chamber) counting to low-geometry (surface barrier detector) counting without disturbing the geometry of the experimental setup.

The measurements were made in a thermal neutron field in three steps. In the first step, both halves were operated as ionization chambers. After extrapolation of the measured pulse-height spectrum to zero pulse height, the counts, $C_f^{2\pi}$, relative to the monitor counts, C_m, are

$$C_f^{2\pi}/C_m = \varepsilon \cdot C_o/C_m,$$

where C_o is the fission rate and ε the counting efficiency. The half of the counter which contains the deposit to be measured was evacuated in the second step and the fission events were detected with the low-geometry counter. The corresponding counts per monitor counts are given by

$$C_f^{LG}/C_m' = \Omega \cdot C_o'/C_m',$$

where Ω is the space angle for the low geometry detector. A typical spectrum obtained with the low-geometry fission counter is shown in Fig. 7. It is assumed that there is no effect on the fissions in the measured deposits per monitor count due to the gas being in one half of the counter instead of the vacuum, i.e.

$$(C_o/C_m)_{gas} = (C_o/C_m)_{vac}.$$

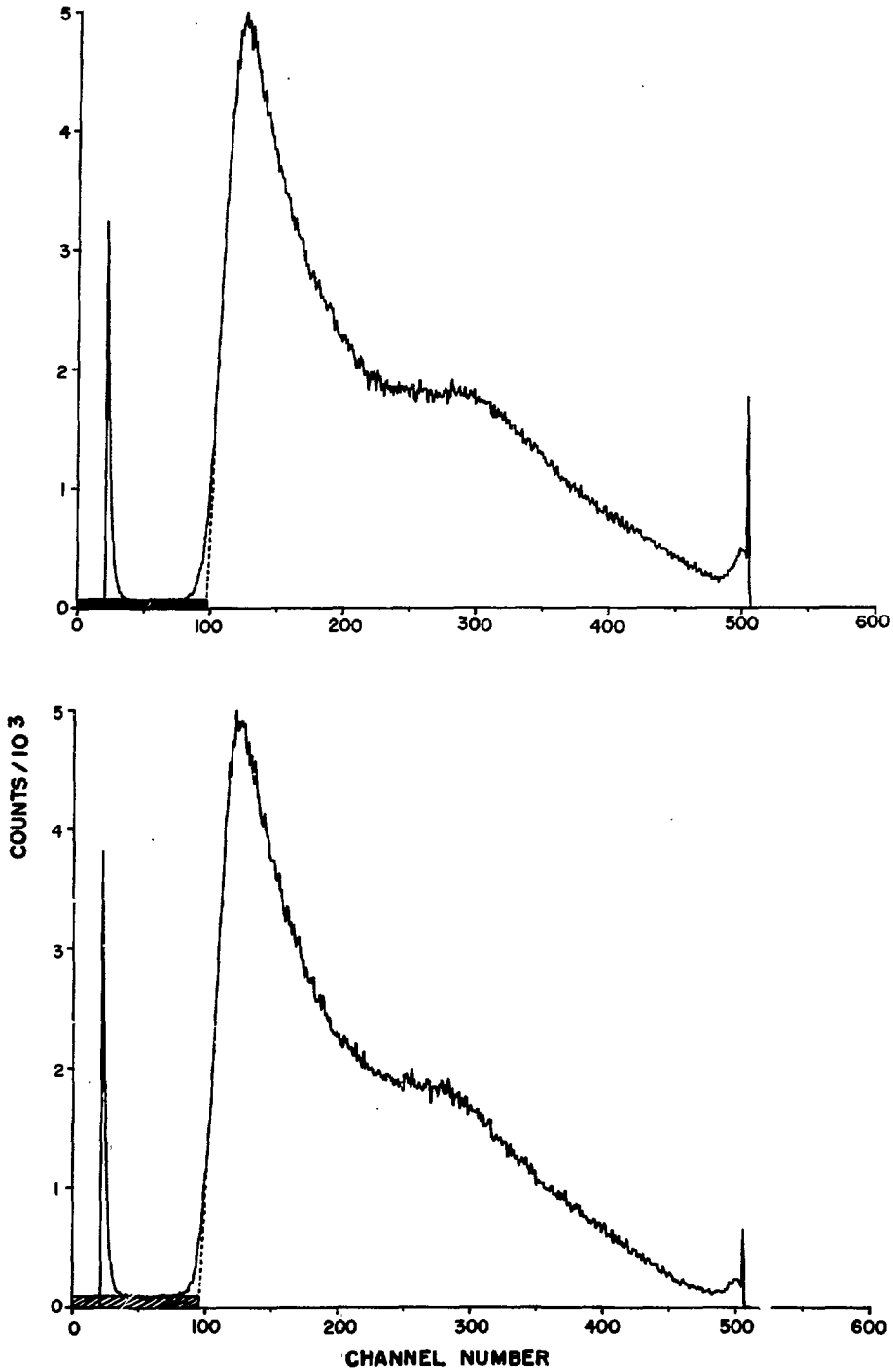

Fig. 5. Comparison of the Fission-Fragment Pulse Height Spectra Obtained for Two Deposits of Similar Thicknesses (The number of pulses below the geometrical cut-off are indicated with the shaded areas.)

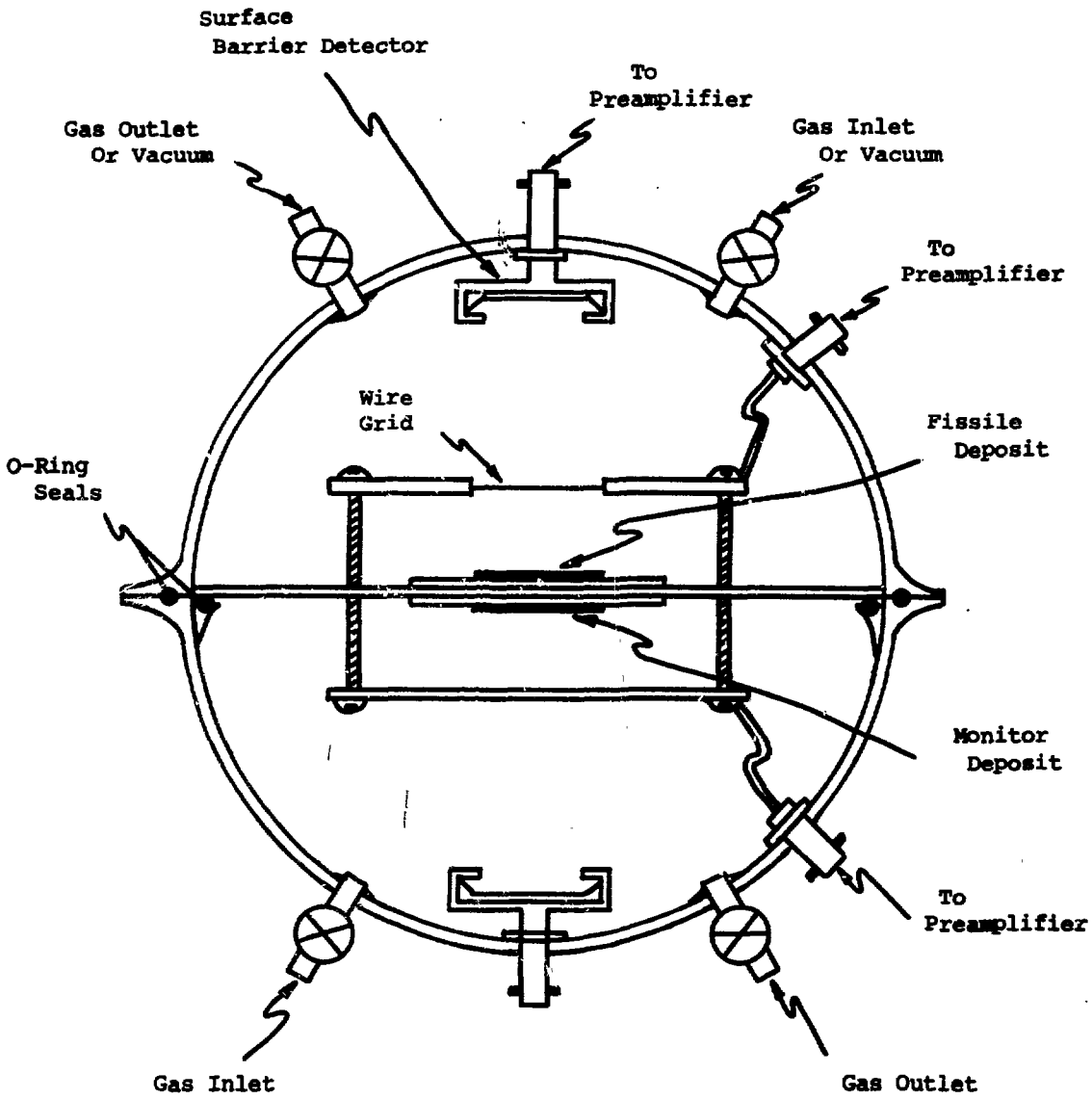

Fig. 6. Schematic of the 2π Ionization/Low-Geometry Counter Designed for the Measurement of Fission Fragment Absorption

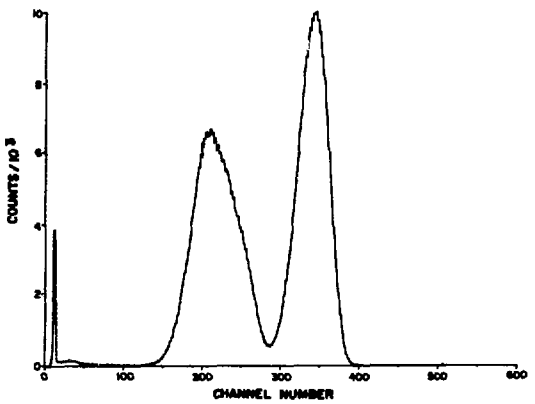

Fig. 7. Fission Fragment Pulse Height Spectrum obtained with the Low Geometry Counter

The fission fragment absorption is therefore obtained from

$$\varepsilon = \Omega \frac{C_f^{2\pi}/C_m}{C_f^{LG}/C_m'} .$$

Because the low-geometry factor was only ~1/100, it was preferred to determine it in the third step of the measurement based upon the known alpha decay rate of the sample, $C_{\alpha o}$. By increasing the gain of the main amplifier, the alpha decay spectrum was measured and the geometry factor was found from

$$\Omega = \frac{C_\alpha}{C_{\alpha o}} .$$

The geometry factor was found to be the same within ±0.15% in all four measurements and the average value was used.

The fission fragment absorption of two ^{235}U deposits and two ^{239}Pu deposits were measured in this way. The results are shown in Figs. 8 and 9. The fission fragment absorption calculated with the formulas given at the beginning of this section are shown by the solid lines in these figures. Uncertainties which contribute to these measurements are due to statistics (0.07-0.10% for the low geometry count rates, 0.08-0.10% for the 2π count rates, 0.08-0.12% for the monitor count rates) and the geometry factor (0.25%, mainly determined by the uncertainties of the alpha decay rates $C_{\alpha o}$). The differences of the fission fragment

absorption correlates reasonably well with the full width at two third maximum of the alpha spectra (FW2/3M) divided by the sample thickness, as well as the fraction of fission fragments below the geometrical cut-off (FFBCO) divided by the sample thickness. This can be seen from Table XI.

The fission fragment absorptions for all samples were finally determined based on the expression

$$\varepsilon = 1 - a \cdot b \cdot t$$

where a is the αFW2/3M or the FFBCO, b is a constant determined as an average from the four measured values and t is the sample thickness. The values for ε are given in Tables XII-XIV. For the ^{235}U and ^{239}Pu deposits, these are the averages of the two determinations. For the ^{238}U deposits, for which the αFW2/3M values were not available, the ε values are based on the FFBCO only. The uncertainties are due to the uncertainties of the measured fission fragment absorptions (Δ_2) and the differences obtained from the two possible values (Δ_1).

IV. MEASUREMENTS OF MASS RATIOS BY FISSION COUNTING

Relative fission ratios were measured for the ^{235}U and ^{239}Pu deposits in a back-to-back ionization counter in the thermal column of a small fast reactor (AFSR). Ratios for the ^{238}U deposits were measured in the fast reactor test assembly ZPPR-12. The back-to-back fission counter used in these measurements has been described in Ref. 1. The effects of gradients of the neutron field in AFSR were

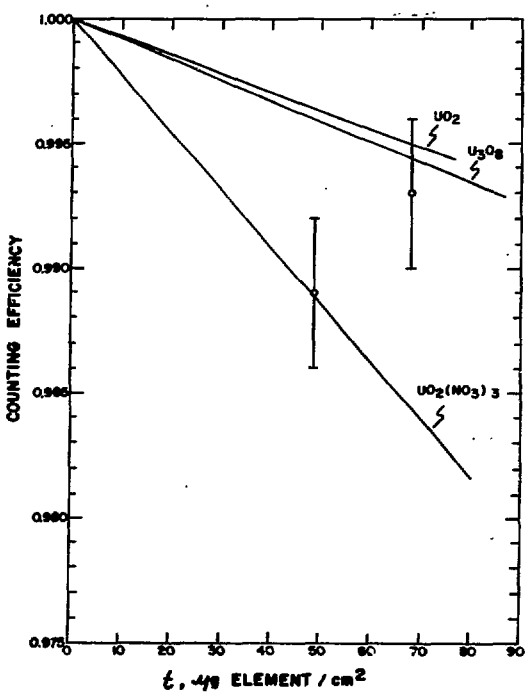

Fig. 8. Fission Fragment Absorption of ^{235}U Deposits

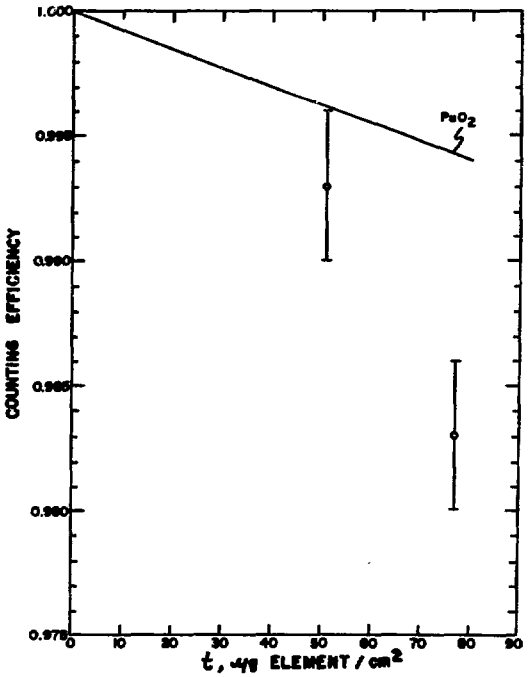

Fig. 9. Fission Fragment Absorption of ^{239} Pu Deposits

TABLE XI. Correlations between Fission Fragment Absorption and Alpha FW2/3M and FFBCO (values in percent)

$(1-\varepsilon)_{*}100/t$	1.4	2.2	2.3	1.0
αFW2/2M/t	1.5	1.9	1.9	1.5
FFBCO/t	1.4	2.1	1.9	1.4

TABLE XII. 2π FF Counting Efficiencies for ^{235}U Samples

Sample	ε	Δ_1/%	Δ_2/%	$\Delta\varepsilon$/%
NEW5-1	0.9909	0.0	0.3	0.30
-2	0.9910	0.0	0.3	0.30
-3	0.9910	0.0	0.3	0.30
-4	0.9918	0.1	0.3	0.32
-5	0.9901	0.1	0.3	0.32
-6	0.9906	0.1	0.3	0.32
-7	0.9903	0.1	0.3	0.32
-8	0.9905	0.1	0.3	0.32
-9	0.9902	0.1	0.3	0.32
-10	0.9905	0.1	0.3	0.32
-11	0.9901	0.0	0.3	0.30
-12	0.9899	0.3	0.3	0.42
-13	0.9879	0.1	0.3	0.32
-14	0.9870	0.2	0.3	0.36
-15	0.9878	0.1	0.3	0.32
-16	0.9879	0.0	0.3	0.30
HAR-A	0.9883	0.1	0.3	0.32
-B	0.9877	0.1	0.3	0.32
OLD5-8	0.9909	0.2	0.3	0.36
-19	0.9890	0.2	0.3	0.36
-22	0.9871	0.2	0.3	0.36
-23	0.9899	0.2	0.3	0.36

TABLE XIII. 2π FF Counting Efficiencies for ^{239}Pu Samples

Sample	ε	Δ_1/%	Δ_2/%	Δε/%
NEW9-5	0.9920	0.2	0.3	0.36
-6	0.9929	0.0	0.3	0.30
-7	0.9927	0.0	0.3	0.30
-8	0.9930	0.1	0.3	0.32
-9	0.9918	0.1	0.3	0.32
-10	0.9893	0.1	0.3	0.32
-11	0.9894	0.2	0.3	0.36
-12	0.9856	0.3	0.3	0.42
-13	0.9843	0.0	0.3	0.30
-14	0.9908	0.2	0.3	0.36
-15	0.9896	0.2	0.3	0.36
-16	0.9861	0.4	0.3	0.50
-17	0.9868	0.1	0.3	0.32
OLD9-65	0.9905	0.3	0.3	0.42
-70	0.9907	0.2	0.3	0.36
ZPR-01	0.9930	0.3	0.3	0.42

TABLE XIV. 2π FF Counting Efficiencies for ^{238}U Samples

Sample	ε	Δ_1/%	Δ_2/%	Δε/%
NEW8-1	0.9891	0.2	0.3	0.36
-2	0.9899	0.2	0.3	0.36
-3	0.9896	0.2	0.3	0.36
-4	0.9881	0.2	0.3	0.36
-5	0.9899	0.2	0.3	0.36
-6	0.9901	0.2	0.3	0.36
-7	0.9902	0.2	0.3	0.36
-8	0.9910	0.2	0.3	0.36
-9	---			
-10	0.9885	0.2	0.3	0.36
-11	0.9884	0.2	0.3	0.36
-12	---			
-13	0.9862	0.2	0.3	0.36
-14	0.9881	0.2	0.3	0.36
-15	0.9888	0.2	0.3	0.36
-16	0.9889	0.2	0.3	0.36

eliminated by turning the fission chamber by 180° after half of the irradiation time. The gradient in ZPPR-12 was known from $^{238}U(n,f)$ reaction rate foil mappings and caused an effect of only 0.04%. The measurements in AFSR used a procedure which has been described in more detail in Ref. 3. A random pulser rate was split on an odd-even basis and added to the signals from the two halves of the back-to-back fission counter. With appropriate tags, the signals were rooted to yield spectra with the following assignments:

Tag 0	Event but missing tag
1	Pulser event but missing chamber half indicator
2	Fission event in detector half 1
3	Pulser event in detector half 1
4	Fission event in detector half 2
5	Pulser event in detector half 2
6	Accidental coincidence between fission events
7	Accidental coincidence between fission events and a pulser event.

The ratios of the pulser events (tags 3 and 5) were found to be within 0.1% of unity, indicating negligible effects of the dead-time in the two branches on the measured ratio. Inappropriate events (tags 0, 1, 6 and 7) were rare (≤0.1-0.2%) and addition of these events to the pulser and fission pulse height spectra changed the resulting ratios by ≤0.1%.

Typical pulse height spectra are shown in Fig. 5. The flat portion at low pulse heights was used for extrapolation to zero pulse height. After correction for the events lost below the electronic threshold (typically 0.5%), the mass ratio is obtained from

$$\frac{m_1}{m_2} = \frac{C_{f1}}{C_{f2}} \frac{\varepsilon_2}{\varepsilon_1} \frac{g_2\hat{\sigma}_2}{g_1\hat{\sigma}_1} \frac{W_2}{A_2} \frac{A_1}{W_1}$$

where the C_{fi} are the measured fission events, the ε_i are the fission fragment counting efficiencies which are determined by the total fission fragment absorption as discussed in the previous chapter, $g_i\hat{\sigma}_i$ are the effective fission cross sections in terms of the Westcott convention,[15] the W_i are the weight percent of the isotope in the material, and the A_i are the atomic weights of the materials. For ratios between deposits of the same material this simplifies to

$$\frac{m_1}{m_2} = \frac{C_{f1}}{C_{f2}} \frac{\varepsilon_2}{\varepsilon_1} .$$

For ratios between deposits with the same principle fissile isotope but different isotopic composition only the $g\hat{\sigma}$ ratio cancels. Two ratios were measured between ^{235}U and ^{239}Pu deposits. The preliminary results from the evaluation of ENDF/B-VI[29] were used for the $g\hat{\sigma}$ ratio:

$$\frac{(g\hat{\sigma})(^{239}Pu)}{(g\hat{\sigma})(^{235}U)} = 1.3835 \pm 0.5\%.$$

Contributions from epithermal neutrons were found to be negligible for both, ^{235}U and ^{239}Pu. The graphite of the thermal column of AFSR came from the reactor CP1 and impurities in this graphite have been identified.[16] These impurities cause a spectrum hardening[17] which in turn required a correction due to the temperature dependence of the g-factors.[15] This correction was 1.4% and was only required for the ratio between the ^{235}U and ^{239}Pu deposits.

The results for the mass ratios based on relative fission counting are given in Tables XV to XVIII.

TABLE XV. Mass Ratios Based on Fission Counting (^{235}U Samples)

Ratio of Samples New5	Mass Ratio	Δ(Stat)[a] %	Δ(FF Abs) %	Δ(Extr) %	Δ(Int) %	Δ (Total) %
2/1 *	1.0139	0.10	0.1	0.1	0.1	0.20
4/3	0.9672	0.15	0.2	0.1	0.1	0.29
5/1	1.4011	0.15	0.2	0.1	0.1	0.29
6/2	1.3696	0.15	0.2	0.1	0.1	0.29
1/7	0.7215	0.16	0.2	0.1	0.1	0.30
2/8 *	0.7335	0.10	0.2	0.1	0.1	0.26
1/9	0.7267	0.16	0.2	0.1	0.1	0.30
2/10*	0.7336	0.10	0.2	0.1	0.1	0.26
1/11*	0.7393	0.09	0.1	0.1	0.1	0.20
2/12*	0.9825	0.10	0.3	0.1	0.1	0.34
1/3	0.9938	0.17	0.1	0.1	0.1	0.24
2/4	1.0395	0.17	0.2	0.1	0.1	0.30
13/14	0.9982	0.16	0.3	0.1	0.1	0.16
15/16	0.9528	0.17	0.2	0.1	0.1	0.30
2/13	0.7344	0.16	0.2	0.1	0.1	0.30
14/15	1.0493	0.17	0.3	0.1	0.1	0.37
3/12	0.9741	0.17	0.3	0.1	0.1	0.37
#19/#22[b]	1.0320	0.17	0.4	0.1	0.1	0.46

*Measured twice with agreement within the statistical uncertainties found.

[a]Uncertainties are for counting statistics (Stat), FF absorption (FF Abs), the extrapolation to zero pulse height (Extr), and the integration procedure used to obtain the ratio from the measured eight spectra (Int.)

[b]OLD5 - deposits.

TABLE XVI. Mass Ratios Based on Fission Counting (^{239}Pu Samples)

Ratio of Samples NEW9	Mass Ratio	Δ(Stat) %	Δ(FF Abs) %	Δ(Extr) %	Δ(Int) %	Δ (Total) %
5/7 *	0.9940	0.11	0.2	0.1	0.1	0.27
5/6	1.0624	0.17	0.2	0.1	0.1	0.30
7/8	1.0446	0.17	0.1	0.1	0.1	0.24
5/9	0.9131	0.16	0.3	0.1	0.1	0.37
7/10	0.9578	0.17	0.1	0.1	0.1	0.24
5/11	0.9142	0.17	0.4	0.1	0.1	0.42
7/12	0.9091	0.16	0.4	0.1	0.1	0.42
5/13	0.7030	0.16	0.2	0.1	0.1	0.30
14/15	0.7882	0.16	0.4	0.1	0.1	0.42
16/17	1.1607	0.16	0.5	0.1	0.1	0.54
15/16	0.9725	0.17	0.5	0.1	0.1	0.55
8/16	0.9440	0.17	0.5	0.1	0.1	0.55
8/13	0.6753	0.15	0.1	0.1	0.1	0.24

*Measured twice with agreement within the statistical uncertainty found.

TABLE XVII. Mass Ratios Based on Fission Counting (^{238}U Samples)

Ratio of Samples NEW8	Mass Ratio	Δ(Stat) %	Δ(FF Abs) %	Δ(Extr) %	Δ(Int) %	Δ (Total) %
5/1	0.9577	0.23	0.4	0.1	0.1	.48
6/2	0.9792	0.24	0.4	0.1	0.1	.49
10/2	0.9469	0.24	0.4	0.1	0.1	.49
14/2	0.9943	0.24	0.4	0.1	0.1	.49
7/2	0.9793	0.24	0.4	0.1	0.1	.49
15/3	1.0001	0.25	0.4	0.1	0.1	.49
8/4	0.9944	0.24	0.4	0.1	0.1	.49
16/4	0.9915	0.25	0.4	0.1	0.1	.49

TABLE XVIII. Mass Ratios from Fission Counting (Different Materials)

Ratio of Samples	Mass Ratio	Δ(Stat) %	Δ(FF Abs) %	Δ(Extr) %	Δ(Int) %	Δ(Therm)[a] %	Δ (Total) %
NEW9-6/OLD9-65	0.9354	0.17	0.3	0.1	0.1		0.37
NEW9-7/OLD9-70	1.0039	0.17	0.2	0.1	0.1		0.30
ZPR-1/NEW9-8	0.7879	0.12	0.4	0.1	0.1		0.44
NEW5-3/NEW9-7	1.1219	0.17	0.1	0.1	0.1	0.5	0.56
NEW5-3/NEW9-9	1.1773	0.17	0.2	0.1	0.1	0.5	0.58
HAR-A/NEW5-1	2.8678	0.11	0.1	0.1	0.1		0.20
NEW5-3/HAR-A	0.3500	0.14	0.1	0.1	0.1		0.22
NEW5-2/HAR-B	0.3512	0.14	0.1	0.1	0.1		0.22
NEW5-2/OLD5-8	1.3912	0.15	0.2	0.1	0.1		0.29
-1 -19	1.0733	0.14	0.2	0.1	0.1		0.28
-3 -22	1.1140	0.16	0.2	0.1	0.1		0.30
-3 -23	1.1154	0.16	0.2	0.1	0.1		0.30

[a]Uncertainties due to thermal cross sections.

V. GENERALIZED LEAST-SQUARES FIT OF THE DEPOSIT MASSES

The masses of the 54 deposits have been overdetermined with 138 measurements. Determinations of each of the masses have been made based on absolute alpha decay rate measurements, determinations of 16 of the deposit masses were available from isotopic dilution analysis, 15 mass ratios were obtained from relative alpha decay rate measurements, and 51 mass ratios were obtained from relative fission ratio measurements. The determinations of the masses based on low-geometry alpha decay rate measurements are partially correlated due to the uncertainties of the geometry factor of the counter. The uncertainty of the specific activity is totally correlated. The mass determinations by isotopic dilution are in part correlated due to the use of the same NBS standards (see Table X). The mass ratios obtained from relative alpha decay rate determinations are correlated due to the statistical uncertainty of the reference deposit (NEW5-1) and in part due to the uncertainties of the counting efficiency correction and the plateau stability. The uncertainty caused by the fission fragment absorption has a large component which is due to the experimental determination of the fission fragment absorption for the four deposits (see chapter III). However, for ratio measurements this uncertainty component cancels and fission ratios between different deposits are largely uncorrelated. Ratios which involve one particular deposit are partially correlated due to the random component of the uncertainty for the fission fragment absorption.

A priori values of the masses were chosen within ~0.2% of the masses determined by absolute alpha counting. Adjustments to these masses were obtained from the well known least-squares equation[19]

$$\delta = (A^T C^{-1} A)^{-1} A^T C^{-1} M$$

where δ is the adjustment vector, A is the coefficient matrix (A^T is its transpose) with the coefficients

$$\frac{\hat{m}_{ik}}{\Delta m_i} \quad \text{for measured masses, and}$$

$$\frac{\hat{R}_{ikl}}{\Delta R_i} \text{ and } -\frac{\hat{R}_{ikl}}{\Delta R_i} \quad \text{for measured mass ratios}$$

$$\text{with } \hat{R}_{ikl} = \frac{\hat{m}_k}{\hat{m}_l}, \quad \hat{m} \text{ being the a priori mass.}$$

C is the correlation matrix of the measurements (C^{-1} is its inverse) and M is the measurement vector with

$$M_i = \frac{m_k - \hat{m}_k}{\Delta m_i} \quad \text{for measured masses, and}$$

$$M_i = \frac{R_{ikl} - \hat{R}_{kl}}{\Delta R_i} \quad \text{for measured ratios,}$$

where $\Delta m_i, \Delta R_i$ are the uncertainties of the measurements. For details on the transformations involved in this particular formulation see Ref. 18. The values obtained from the least-squares fit for the 54 deposit masses and their uncertainties are given in Table XIX. The square root of the χ^2 per degree of freedom of the measured values is 0.44. Thus, the usually recommended scaling of the covariance matrix of the result[19] would further reduce the uncertainties given in Table XIX by this factor, but has not been done here.

VI. DETERMINATION OF ^{238}U CAPTURE RATES IN METALLIC FOILS

The ^{238}U capture rate in depleted uranium samples irradiated in ZPPR are determined by detecting the 278 KeV gamma,[5] which occurs in the decay of ^{239}Np, with a Ge(Li)-detector. The calibration of the detector efficiency, including the branching for the 278 KeV transition, has been determined by measuring the intensity of this gamma transition for an ^{243}Am source with a well known alpha decay rate. This calibration procedure is referred to as the ^{243}Am calibration technique. The specific procedure used for capture rate measurements in ^{238}U samples in ZPPR has been described in Ref. 1 and is referred to as the "standard procedure". Several other techniques have been used in the past in order to check this standard procedure.[1] As some of the values used in the analysis of these additional measurements have changed, the updated values are given at the end of this section.

Two new measurements were carried out in order to check the calibration of the standard ^{238}U capture rate determination procedure. Metallic depleted uranium samples (discs with diameters of 1.27 cm and 0.0127 cm thick, sandwiched between two 0.0019 cm thick aluminum foils) were irraidated in the thermal column of AFSR sandwiched between two fissile deposits in the back-to-back fission counter. In one irradiation, two of the new ^{235}U deposits were used and in a second irradiation of another depleted uranium sample, two of the new ^{239}Pu deposits were used. The fission events were recorded in the manner described in Section IV. The total number of fission counts obtained by adding all fission spectra counts and correcting for deadtime based on the life-time of the analyzer agreed to better than 0.1% with the counts obtained with the dead-time correction based upon the recorded pulser rates. After a sufficient time delay for the ^{239}U to decay to ^{239}Np, the capture events in ^{238}U were determined by the standard ZPPR procedure. The capture rate was also determined with a second Ge(Li)-detector for which an independent calibration with different ^{243}Am sources was carried out.

The number of ^{238}U capture events per gram of ^{238}U, C_s, is given by

$$C_s = \frac{T \cdot C_\gamma}{W_s \cdot \varepsilon_\gamma a_\gamma \cdot F \cdot k} = \frac{C_f}{\varepsilon_f} \frac{A_f}{A_s} \frac{\sigma_s g_s(T)}{\sigma_f g_f(T)} \cdot \frac{1}{W_f} \cdot \frac{S_s}{S_f} \frac{E_s}{E_f}$$

TABLE XIX. Results from the LS-Fit for the Deposit Masses

Deposit	Mass, μg	Uncertainty, %
NEW9-05	106.84	0.16
06	100.62	0.17
07	107.47	0.14
08	102.65	0.14
09	115.61	0.13
10	111.18	0.12
11	116.42	0.13
12	117.46	0.11
13	152.32	0.09
14	83.58	0.14
15	105.81	0.11
16	108.35	0.16
17	93.35	0.16
ZPR-01	81.13	0.19
OLD9-65	107.38	0.15
70	107.37	0.15
NEW5-01	119.82	0.18
02	121.70	0.15
03	120.43	0.15
04	116.74	0.18
05	167.96	0.13
06	116.53	0.11
07	166.07	0.11
08	164.99	0.10
09	164.83	0.09
10	165.14	0.11
11	162.02	0.15
12	123.25	0.13
13	165.07	0.07
14	164.52	0.07
15	156.57	0.06
16	164.11	0.06
OLD5-08	86.87	1.06
19	110.79	0.83
21	107.12	0.86
22	106.94	0.86
HAR-A	346.23	0.04
B	346.93	0.05

TABLE XIX (cont'd)

Deposit	Mass, μg	Uncertainty, %
NEW8-01	136.28	0.11
02	131.33	0.11
03	131.94	0.11
04	130.14	0.11
05	130.27	0.11
06	128.05	0.12
07	128.64	0.11
08	129.39	0.11
09	128.98	0.11
10	123.95	0.11
11	132.31	0.10
12	128.86	0.11
13	130.04	0.08
14	129.13	0.08
15	131.22	0.07
16	129.21	0.07

where T is the time of the irradiation, C_γ is the number of counts in the 278 KeV gamma ray peak, W_e is the ^{238}U mass of the depleted uranium sample, $\varepsilon_\gamma a_\gamma$ are the detector efficiency and gamma branching for the 278 KeV gamma ray, F is a factor depending on the irradiation time, delay time, counting time and the half-lives of ^{239}U and ^{239}Np (see Ref. 20) and k is a correction for the time dependence of the neutron flux during the irradiation[20] which was determined with a power monitor and found to be very close to unity (0.99996).

C_f is the number of counts obtained from the recorded fission fragment pulse-height spectra and extrapolation to zero pulse-height, ε_f is the fission fragment counting efficiency (see section III), the A's are the atomic weights, the $\sigma \cdot g(T)$ are the thermal cross sections and (temperature dependent) g-factors according to the Westcott convention,[15] and W_f is the mass of the fissile deposits. The S's and E's are corrections for self-shielding and for reactions due to epithermal neutrons. Thus, C_e can be determined by both, the left-hand side of the above equation using the ^{243}Am calibration technique, and by the right-hand side assuming known thermal cross sections.

The new measurements based on the ^{243}Am technique were carried out as described in detail in Refs. 20 and 21. The alpha decay rates of two ^{243}Am samples were determined based upon counting on several shelves of the low-geometry alpha counter. One of the ^{243}Am samples was made from the same material used previously,[21] i.e. it was contaminated with ^{241}Am, ^{242}Cm and ^{244}Cm but the second sample was made from a material specifically purified in order to assure the absence of ^{243}Cm which cannot be distinguished in the alpha spectrum but feeds the same level in ^{239}Pu which decays by the emission of the 278 KeV gamma ray. The agreement for

the counting efficiency and branching ($\epsilon_\gamma a_\gamma$) obtained for the two sources was within ± 0.16% which is consistent with counting statistics, positioning accuracy, and the uncertainty of a correction required for a slightly different diameter of the high-purity ^{243}Am source.

The combined effects of gamma ray attenuation under oblique angles and of sum coincidences were measured by obtaining the count rates for the ^{243}Am source once being at the front surface of an unirradiated depleted uramium sample and once at the back surface, i.e. with the uranium sample as an absorber between the source and the detector. The difference beteeen this approximation and the efficiency of counting a homogeneously activated uranium sample was obtained from Monte Carlo calculations.[21] The latter correction was smaller (0.1%) than previously obtained [21] due to a larger distance between the sample and the detector (~3 cm) and a cadmium sheet between the sample and the detector which reduced the counting efficiencies for the lower-energy gamma rays and thus reduced the sum coincidence effect. The uncertainties of the determination of C_s based on this new ^{243}Am calibration measurement are summarized in Table XX.

The thermal cross sections and g-factors for 20°C were taken from the preliminary evaluation of ENDF/B-VI.[29] The temperature dependence of the g-factors by Westcott[15] were used in order to correct for the effective temperature in the impurities-containing graphite (see Section IV). The self-shielding factors, including a correction for the edge effect of the depleted uranium sample, were calculated as described in Ref. 17. The fissile deposit had a diameter of ~1.78 cm with an area larger than the area of the depleted uranium sample by about a factor of

TABLE XX. Uncertainties Associated with the New ^{243}Am Calibration for ^{238}U Capture Rate Measurements

Determination of $\epsilon_\gamma a_\gamma$	
Alpha Counting Statistics	0.12%
Alpha Counter Geometry	0.10%
Gamma Counting Statistics	0.06%
Sample Absorption Measurement	
Gamma Counting Statistics	0.17%
Positioning Uncertainty	0.20%
Monte Carlo Correction	0.05%
^{238}U Capture Measurement	
C_γ Statistics	0.17%
T/F, and k	0.17%
W_s	0.10%
Total Uncertainty	0.41%

2. The self-shielding of the fissile deposits was therefore taken as an area-weighted average between negligible self-absorption for the non-overlapping area and the self-absorption for the overlapping area. A small correction (0.25% ± 0.30%) was applied for the flux gradient based upon prior measurements with ^{238}U foils in the same location of the thermal column.

Flux perturbations due to the samples[17] were assumed to be the same for the ^{238}U capture and the fission rates.

The total capture rate in ^{238}U is given by[17]

$$C = C_{th} + C_{epi}$$
$$= C_{th}(1 + F_{Cd}C_{Cd})$$

where C_{th} is the capture due to the Maxwellian spectrum and C_{epi} is due to the (cut-off) 1/E slowing down spectrum. C_{Cd} is the cadmium ratio which was measured in the location in which the irradiations were made with a depleted uranium sample inside a ~0.05 cm thick cadmium capsule. This ratio was found to be 0.019. F_{Cd} is a correction which takes into account the cadmium cut-off energy on the epithermal neutron flux and is typically 1.1 - 1.3.[17] A value of 1.15 has been used and a large uncertainty for this value (±0.2) has been accepted because of the small impact of this correction due to the low value of C_{Cd}. Corresponding corrections for the ^{235}U and ^{239}Pu fission rates are negligible because of their large thermal cross sections which are comparable to their resonance integrals, which is not the case for ^{238}U capture. The uncertainties contributing to the determination of C_s based upon the thermal calibration are given in Table XXI.

The results from the new ^{243}Am measurements and from the thermal calibration technique are given in Table XXII relative to the standard measurement technique.

An earlier measurement of the capture in ^{238}U was based upon the determination of the Ge(Li)-detector efficiency with a ^{203}Hg standard source from NBS and the emmission probability for the 278 KeV gamma ray in the decay of ^{239}Np. Current values for the latter are shown in Table XXIII. The use of the weighted average of these values instead of the previously used 14.1% results in the difference relative to the standard technqiue shown in Table XXII.

The ^{238}U capture has also been measured at ANL-East using a radiochemistry technique which consists of chemically separating the ^{239}Np together with a ^{237}Np tracer and measuring the ^{239}Np decay through an aluminum absorber with an end window proportional counter. (The ^{237}Np tracer and alpha counting is used to determine the chemical yield of the ^{239}Np separation.[28]) An intercomparison between ANL-East and ANL-West made for 10 samples resulted in a negligible difference of <0.03%, thus the difference between the radiochemistry method and the standard measurement technique at ZPPR can be concluded to be the same as observed at ANL-East which has been stated in Table XXII.

TABLE XXI. Uncertainties Associated with the Thermal Calibration Technique for Capture Rate Measurements

Cross Sections and g Factors	
^{238}U σ	0.41%
g (20°C)	0.10%
^{235}U σ	0.25%
g (20°C)	0.11%
^{239}Pu σ	0.33%
g (20°C)	0.28%
^{235}U g(T)/g(20°C)	0.40%
^{239}Pu g(T)/g(20°C)	1.00%
Fission Counting	
Mass	0.20%
Statistics	0.05%
Extrapolation	0.10%
Dead-time	0.10%
ε_f	0.30%
Corrections	
Self-shielding	0.20%
Epithermal Capture	0.20%
Edge Effect	0.20%
Total Uncertainty	0.83%(^{235}U) - 1.28%(^{239}Pu)

TABLE XXII. Differences of Various ^{238}U Capture Rate Measurement Techniques Relative to Standard Technique

Hg Calibration	+0.7 ± 1.1%
Radiochemistry	+0.1 ± 0.7%
Mass Spectrometry	+1.9 ± 0.5%
Present Measurements	
^{243}Am Calibration	+0.49 ± 0.41%
Thermal Calibration	+0.25 ± 1.06%

TABLE XXIII. 278 KeV Gamma Emission per ^{239}Np Decay

	Percent
Ewan, 1958[22]	14.076 (±0.4)*
Ahmad and Wahlgreen, 1972[23]	14.5 ± 0.4
Yurova et al., 1974[24]	14.1 ± 0.4
Starozhakov et al., 1977[25]	15.0 ± 0.5
Ahmad, 1982[26]	14.5 ± 0.4
Chang Yongfu et al., 1983[27]	14.21 ± 0.13
Average	14.275 ± 0.091

*Assumed uncertainty.

Another intercomparison in which both ANL-East and ANL-West were involved was based upon the mass spectrographic determination of the ^{239}Pu resulting from capture in ^{238}U.[28] The value given in Table XXII is the average between the results obtained at ANL-East and ANL-West, again taking into account the zero bias between the ZPPR standard measuring technique and the GE(Li) detector measurements at ANL-East.

VII. DISCUSSION AND CONCLUSIONS

New reference fissile and fissionable deposits have been established for ^{235}U, ^{239}Pu and ^{238}U. The masses of these samples have been established with better than 0.2% uncertainties based upon multiple overdeterminations by absolute alpha counting, isotopic dilution and relative alpha and fission counting. The measured values are consistent with the values obtained from the generalized least-squares fit which is reflected in the χ^2 value of 0.44. This improves the uncertainties of the knowledge of the sample masses by a factor of 6 compared with the old reference deposits which have been used the last ~17 years. Some of the old reference deposits were invovled in the present measurements and masses lower by 1.4 - 2.5% were found for the ^{235}U and ^{239}Pu deposits. Whereas the new values for the ^{239}Pu masses of the old reference deposits are rather reliable, the uncertainties of the ^{235}U masses of the old reference deposits remains large due to the large uncertainty of the isotopic composition of that material and uncertainties of the fission fragment absorption.

Two new measurements of the capture rate in depleted uranium samples confirm the measurement technique used at ZPPR for ^{238}U(n,γ) within the typical uncertainty of ±0.5%. Only one[28] of several checks made on this measurement procedure suggests a difference outside of the estimated uncertainties and it is therefore likely that the problem was in that particular measurement. This seems to be supported by the differences in the results obtained at ANL-East and ANL-West which was contrary to a very good agreement obtained for a direct intercomparison of the ^{238}U capture rate determination of 10 foils.

ACKNOWLEDGEMENT

The authors wish to express their appreciation to the people who provided the absolute mass and isotopic analyses of the uranium and plutonium samples. At the New Brunswick Laboratory, separations and sample preparation were performed by R. D. Oldham and mass spectrometric analyses by D. Crawford. In the Analytical Chemistry Laboratory of the Chemical Technology Division, separations and sample preparation were performed by A. Essling and mass spectrometric analyses by E. Rauh and D. G. Graczyk. In the Analytical Chemistry Laboratory at ANL-E, separations and sample preparation were performed by J. O. Young and mass spectrometric analyses by M. T. Laug and H. E. Keckler. The measurements provided by these people were very important to this work.

REFERENCES

1. S. B. Brumbach and D. W. Maddison, "Reaction Rate Calibration Techniques at ZPPR for ^{239}Pu Fission, ^{235}U Fission, ^{238}U Fission, and ^{238}U Capture," Argonne National Laboratory Report ANL-82-38 (1982).

2. W. P. Poenitz et al., "^{235}U Fission Mass and Counting Comparison and Standardization," Argonne National Laboratory Report, Nuclear Data and Measurements Series, ANL/NDM-48 (1979).

3. W. P. Poenitz and J. W. Meadows, "^{235}U and ^{239}Pu Sample-Mass Determinations and Intercomparisons," Argonne National Laboratory Report, Nuclear Data and Measurements Series, ANL/NDM-84 (1983).

   See also: Proc. IAEA Consultants' Meeting on the ^{235}U Fast-neutron Fission Cross Section, Smolenice, INDC(NDS)-146, p. 27 (1983), and Proc. IAEA Advisory Group Meeting on Nuclear Standard Reference Data, Geel, IAEA-TECDOC-335, p. 485 (1984).

4. D. W. Maddison, private communication, Argonne National Laboratory (1984).

5. S. B. Brumbach, private communication, Argonne National Laboratory (1985).

6. C. W. Reich, Proc. IAEA Advisory Group Meeting on Nuclear Standard Reference Data, Geel, IAEA-TECDOC-335, p. 390 (1984).

7. W. P. Poenitz and R. J. Armani, J. Nucl. Energy 26, 483 (1972).

8. E. L. Callis, Proc. 25th Conf. on Analytical Chemistry in Energy Technology, Ann Arbor Science, Ann Arbor, MI, p. 115 (1982).

9. R. J. Armani, private communication, Argonne National Laboratory (1985).

10. J. M. Alexander and M. F. Haydek, Phys. Rev. 120, 874 (1960).

11. J. B. Niday, Phys. Rev. 121, 1471 (1961).

12. P. H. White, J. Nucl. Energy A/B19, p. 325 (1964).

13. J. W. Meadows, Proc. Conf. on Nuclear Cross Sections for Technology, NBS Special Publication NBS 594, p. 479 (1979). See also: Nucl. Sci. Eng. 85, 271 (1983).

14. C. Budtz-Jorgensen and H. H. Knitter, Nucl Sci. Eng., 86, 10 (1984).

15. C. H. Westcott, "Effective Cross Section Values for Well-Moderated Thermal Reactor Spectra," Atomic Energy of Canada Report, CRRP-787, (1958).

16. M. M. Bretscher, private communication, Argonne National Laboratory (1985).

17. K. H. Beckurts and K. Wirtz, "Neutron Physics," Springer (1964).

18. W. P. Poenitz, "Data Interpretation, Objective Evaluation Procedures and Mathematical Techniques for the Evaluation of Energy-Dependent Ratio, Shape and Cross Section Data," Proc. Conf. on Nuclear Data Evaluation Methods and Procedures, Brookhaven National Laboratory, September 22, 1980, BNL-NCS-51363, Vol. 1, 249 (1981).

19. S. L. Mayer, "Data Analysis for the Scientists and Engineers," John Wiley and Sons, Inc., New York (1975).

20. W. P. Poenitz et al., "Measurements of the ^{238}U (n,γ) Cross Section at Thermal and Fast Neutron Energies," Nucl. Sci. Eng., 78, 239 (1981).

21. G. J. DiIorio and W. P. Poenitz, "Accurate ^{238}U Neutron Capture Rate Determiantions," Nucl. Inst. and Meth. 198, 461 (1982).

22. G. Ewan et al., Phys. Rev. 116, 950 (1959).

23. J. Ahmad and M. Wahlgram, Nucl. Instr. and Meth. 99, 333 (1972).

24. L. N. Yurova et al., Atomic Energy 36, 51 (1974).

25. D. I. Starozhukov et al., Atomic Energy 42, 219 (1977).

26. J. Ahmad, Nucl. Instr. and Meth. 193, 9 (1982).

27. Chang Yongfu et al., Proc. Conf. on Nuclear Data for Basis and Applied Science, Santa Fe, May 1985, Vol. 1, p. 771, Gordon and Breach Science Publishers.

28. J. M. Gasidlo et al., "A Comparison of Gamma Counting and Mass Spectrometer Measurements for ^{238}U Capture," TANSAO41-1-712 p. 575 (1982).

29. A. D. Carlson et al., Proc. Conf. on Nuclear Data for Basis and Applied Science, Santa Fe, May 1985, Vol. 2, p. 1429, Gordon and Breach Science Publishers.

Distribution for ANL-87-5

Internal:

P. I. Amundson
R. J. Armani
C. L. Beck
E. S. Beckjord
E. F. Bennett
S. K. Bhattacharyya
M. M. Bretscher
S. B. Brumbach
S. G. Carpenter
Y. I. Chang
P. J. Collins
E. K. Fujita
J. M. Gasidlo
R. W. Goin
H. A. Harper
R. N. Hwang
R. E. Kaiser
L. G. LeSage
D. W. Maddison
H. F. McFarlane
R. D. McKnight
D. N. Olsen
W. P. Poenitz (25)
R. W. Schaefer
C. E. Till
D. C. Wade
T. J. Yule
ANL Patent Dept.
ANL Contract File
ANL Libraries (2)
TIS Files (6)

External:

DOE-TIC, for distribution per UC-79d (101)
Manager, Chicago Operations Office, DOE
Director, Technology Management, DOE-CH
Director, DOE-RRT (2)
President, Argonne Universities Association
A. D. Carlson, National Bureau of Standards

Applied Physics Division Review Committee:
M. J. Driscoll, Massachusetts Inst. Technology
W. E. Kastenberg, University of California
R. L. Hellens, C-E Power Systems Combustion Eng. Inc.
D. A. Meneley, University of New Brunswick
H. F. Jackson, Los Alamos National Laboratory
N. J. McCormick, University of Washington